Available online at www.sciencedirect.com
SCIENCE DIRECT®
C. R. Geoscience 336 (2004) 445–454
COMPTES RENDUS GEOSCIENCE

Tectonics

Hydromechanical behaviour of fine-grained calcilutite and fault gouge from the Aigion Fault Zone, Greece

Insun Song *, Stephen C. Elphick, Nicolas Odling, Ian G. Main, Bryne T. Ngwenya

School of GeoSciences, University of Edinburgh, EH9 3JW, Scotland, UK

Received 17 November 2003; accepted after revision 24 November 2003

Written on invitation of the Editorial Board

Abstract

This paper presents the experimental characterisation of hydraulic and mechanical properties of two fine-grained materials from the Aigion Fault Zone, on the southern shore of the Gulf of Corinth, Greece. One is a calcilutite, which commonly caps the basal limestone units, and the other is siliceous active fault gouge from 760 m depth in the borehole. Oedometric compaction/consolidation tests of unconsolidated cylindrical samples at variable stresses were conducted under drained conditions, and then permeability measured by a constant flow technique. The axial strain measurements show consolidation curves with a decelerating strain rate that can be approximated by a power-law function. The permeability is negatively and linearly correlated to the stress, and ranges from 9 to 15×10^{-18} m^2 for the calcilutite and 0.9 to 2×10^{-18} m^2 for the fault gouge with varied vertical stresses. ***To cite this article: I. Song et al., C. R. Geoscience 336 (2004).***

Résumé

Comportement hydromécanique d'une calcilutite et d'une gouge de faille, de granulométrie fine, provenant de la zone de la faille d'Aigion, Grèce. Les propriétés mécaniques et hydrauliques de deux roches granulaires provenant de la zone de la faille d'Aigion (golfe de Corinthe, Grèce) ont été étudiées en laboratoire. Ces deux roches se caractérisent par une petite taille de grains, mais proviennent d'environnements géophysiques différents. La première est une calcilutite de surface, la seconde est une roche silicatée provenant de la zone de glissement située à 760 m de profondeur. Pour des échantillons cylindriques et différentes valeurs de la contrainte verticale, des tests de compaction–consolidation avec drainage ont précédé des mesures de perméabilité à débit constant. La déformation axiale indique un mécanisme de consolidation, et les taux de déformation semblent varier suivant une loi en puissance. La perméabilité est linéairement corrélée à la contrainte et varie de 9 à 15×10^{-18} m^2 pour les échantillons de calcilutite et de 0,9 à 2×10^{-18} m^2 pour les échantillons de roche provenant de la zone de glissement. ***Pour citer cet article : I. Song et al., C. R. Geoscience 336 (2004).***

Keywords: Aigion; calcilutite; gouge; permeability; consolidation

Mots-clés : Aigion ; calcilutite ; gouge ; perméabilité ; consolidation

* Corresponding author.
E-mail address: insun.song@ruhr-uni-bochum.de (I. Song).

1631-0713/$ – see front matter
doi:10.1016/j.crte.2003.11.019

Version française abrégée

Cet article présente une caractérisation expérimentale des propriétés hydrauliques et mécaniques de deux matériaux à grains fins de la zone de la faille d'Aigion, sur la côte sud du golfe de Corinthe. L'un est une calcilutite, qui se trouve entre le banc de calcaire micritique de la base et les dépôts des terrasses marines, composés essentiellement de conglomérats, et l'autre est une gouge siliceuse de la faille active d'Aigion, prélevée à 760 m de profondeur dans le puits de forage d'Aigion (AG-10). La calcilutite peut contrôler la connectivité hydraulique entre le calcaire et les conglomérats et c'est un excellent analogue pour une cataclasite à grains fins, telle qu'on la trouve dans les failles régionales majeures à travers les séquences calcaires. Dans le puits de forage (AG-10) lui-même, la faille active traverse une séquence de radiolarites dans le calcaire, de sorte que la comparaison des propriétés de la calcilutite et de la gouge de faille siliceuse prélevée nous renseigne sur le couplage hydromécanique local et régional dans la faille d'Aigion.

Des échantillons non consolidés ont été remaniés en une carotte cylindrique (diamètre 38 mm, longueur 40 mm) sous faible compaction, puis placés dans une cellule oedométrique avec, à chaque extrémité, des disques en acier inoxydable pareux. Un chargement vertical par palier a été appliqué à l'aide d'un piston hydraulique muni d'un système à accumulateur de gaz dans le bâti de chargement. La perméabilité de l'échantillon a été mesurée à partir de mesures de pression différentielle à travers l'échantillon durant une injection de fluide à vitesse constante. Le tassement de l'échantillon a été mesuré par des capteurs LVDT montés sur les pistons de chargement de la cellule oedométrique. Les mesures du tassement et de la perméabilité ont été effectuées à chaque niveau de chargement axial, de façon à évaluer le comportement hydromécanique des échantillons en fonction de l'épaisseur du recouvrement.

Les analyses par diffraction des rayons X ont montré que les échantillons de calcilutite sont constitués essentiellement de calcite (82 %), de quartz (10 %) et de minéraux argileux en faibles teneurs, et que la gouge de faille est constituée essentiellement de quartz (70 %), d'albite (10 %) de muscovite (12 %) et de traces d'autres matériaux. La taille des particules de l'échantillon de calcilutite est assez étalée et comprise entre 0,4 et 146 µm, avec un diamètre moyen de 15,97 µm. L'échantillon de gouge de faille a une granulométrie encore plus étalée, avec des tailles de particules entre 0,4 et 3600 µm et une moyenne de 490 µm. Cependant, la distribution de la gouge de faille est multimodale, et on s'attend à ce que le comportement hydraulique soit dominé par les fractions les plus fines, alors que les matériaux plus grossiers contribuent à la tortuosité de l'écoulement. À partir de la relation entre le poids spécifique mesuré et le poids spécifique calculé à partir du poids unitaire de chaque constituant, on détermine l'indice des vides et la porosité, qui sont respectivement de 0,58 et 36,9 % pour l'échantillon de calcilutite et de 0,32 et 24 % pour la gouge de faille.

En ce qui concerne la déformation mécanique, les deux échantillons montrent clairement un comportement transitoire lors de changements soudains du chargement externe. Cependant, la calcilutite montre un comportement qui dépend plus du temps et la gouge de faille un comportement qui dépend plus de la pression, cette dernière étant sensible à de petites perturbations du chargement. Nos essais ont également montré que le tassement à un instant donné est une fonction linéaire de la contrainte externe pour les deux échantillons, avec la même dépendance, mais avec une déformation initiale différente. En ce qui concerne les caractéristiques hydrauliques, tous deux montrent une dépendance linéaire et négative entre la perméabilité et la contrainte, allant de 9 à 15×10^{-18} m^2, pour la calcilutite, à 0,9 à 2×10^{-18} m^2, pour la gouge de faille. L'évolution de la perméabilité en fonction de la porosité est approchée pour les deux échantillons par une fonction linéaire dans une double échelle logarithmique. La faible perméabilité des deux échantillons implique que les matériaux à grains fins font barrière à l'écoulement, en comparaison des bancs calcaires lourdement fracturés environnants.

Les valeurs de perméabilité pour la calcilutite sont des valeurs globales qui ne dépendent pas du cisaillement, alors que celles de la gouge siliceuse sont des limites locales sous écoulement et doivent dépendre de la vitesse de cisaillement. Nous concluons que la réponse transitoire à des changements soudains de la contrainte effective peut jouer un rôle crucial dans l'activation dépendant du temps du mouvement de la faille dans la région d'Aigion.

1. Introduction

The Gulf of Corinth in central Greece is an active neotectonic basin formed by two opposed facing normal fault zones striking WNW–ESE at the northern and southern bounds (Fig. 1). Two tectonic processes dominate basin formation. One is a north–south-extension rifting of 11–16 mm yr^{-1} [1], the other is isostatic compensation with footwall uplift from erosion of horsts and hangingwall subsidence due to the sedimentation on the basin [8]. These combined tectonic activities have resulted in intermittent catastrophic slips along the faults in the form of earthquakes, the latest a $M^s = 6.2$ earthquake, in 1995 [3].

The geology of the study area consists mainly of a thick formation of tight, highly fractured micritic limestone as a bedrock, overlain by Late Pleistocene marine terrace deposits, composed mainly of conglomerate. Separating the two sequences is commonly a laminated calcitic mud (properly, 'calcilutite') up to several metres in thickness, providing an unconformable ductile top cap for the limestones. In other areas, the separation between limestone and conglomerate is marked by siliceous radiolarian cherts.

The calcilutite is important both because it can control the hydraulic connectivity between limestone and conglomerate, and because it is an excellent analogue for fine-grained cataclasite expected to be found on major regional faulting through the limestone sequence. Hence its properties are important for the understanding of the hydromechanical response of the Aigion Fault Zone. Within the Aigion borehole (AG-10) itself, the active fault transects the radiolarian cap sequence, so that comparison of material properties of calcilutite and recovered siliceous fault gouge provides insight into both local and regional hydromechanical coupling in the Aigion fault.

2. Experimental program

Calcilutite was sampled from a roadcut outcrop west of the Selinoutas River, 4 km south of the Aigion Fault Zone (Fig. 1). Fault gouge was obtained from 760 m below ground level in the AG-10 well at the intersection with the Aigion Fault [4]. Remoulded materials were used for the tests, with the full size distribution used for calcilutite. The remoulded fault gouge, kindly supplied by Sulem, CERMES Paris, was a sample reconstituted from original fault gouge in the correct particle binnings, but with all material >2 mm diameter removed.

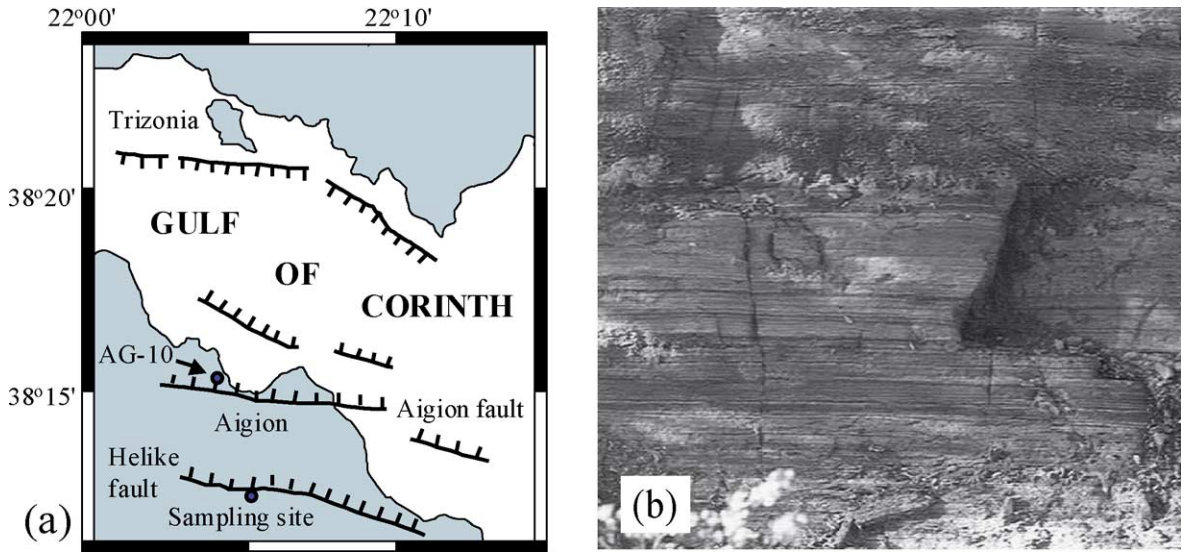

Fig. 1. (**a**) Locations of wellbore (AG-10) and (**b**) calcilutite sampling site.

Fig. 1. Localisation du puits (AG-10) et site d'échantillonnage de la calcilutite.

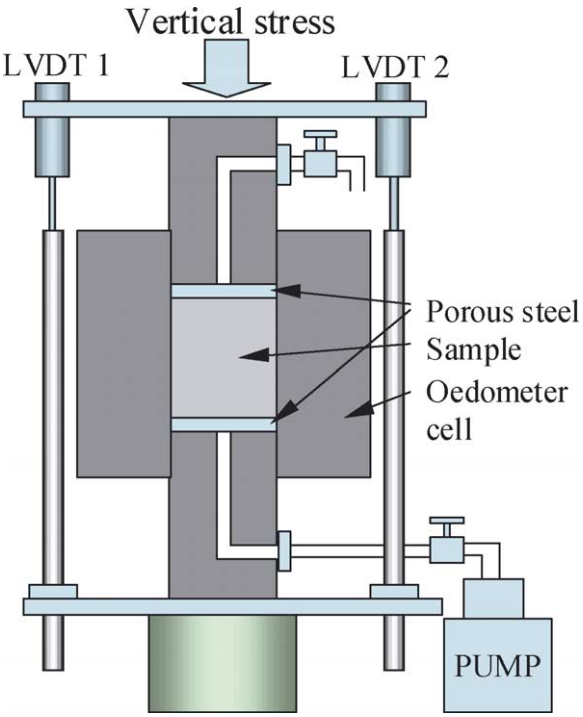

Fig. 2. Schematic of the uniaxial consolidation apparatus.

Fig. 2. Schéma de l'appareil uniaxial de consolidation.

Compaction tests were performed in a solid, opposed piston oedometric cell, shown in Fig. 2. The 38 mm-diameter samples, 3–4 cm long, were preformed in a mould, and wrapped radially in two layers of thin Teflon tape, which decoupled frictional binding between sample and cell wall. Samples were capped at either end with porous stainless steel frit discs. Loading was applied using a gas-accumulator-buffered hydraulic piston in a load frame. Sample compaction was monitored by averaging a pair of gauge LVDTs mounted across the load pistons of the oedometer cell. Thermal pressure cycling in the hydraulic load system was mitigated by water-bath temperature stabilisation of the gas accumulator system, with loading constant to within $\pm 0.5\%$.

Tests commenced with the saturated sample assembly in a drained condition subjected to a constant axial stress. After one or two days of drained consolidation at conditions of zero input flow, water was pumped upward through the sample at a constant rate of 1.05×10^{-10} $m^3 s^{-1}$ for the calcilutite and 4.2×10^{-11} $m^3 s^{-1}$ for the fault gauge. The resulting pressure difference across the sample was used to estimate the permeability using Darcy's law. Tests took at least 48 h for the calcilutite, and 72 h for the fault gouge, due to their different properties. The compaction/permeability cycle was repeated at steps of increasing axial load to obtain the hydromechanical behaviour of the samples as a function of overburden thickness.

After the last stage of the test at 27 MPa vertical stress for the calcilutite, and at 25 MPa vertical stress for the fault gouge, sample relaxation was measured for 24 h after sample-load release. The wet specimen was removed from the cell, weighed, measured, then dried at 105 °C for 48 h, re-weighed and remeasured. The mineral composition and particle size were analysed using X-ray diffraction and laser-diffraction particle size analysis.

3. Sample properties

The particle size of the calcilutite sample ranges from >0.4 to 146 μm, with an average of 15.97 μm in diameter. According to British Standards for particle size ranges [3], it comprises 74% silt size particles, 21% clay size, and 5% fine sand. The reconstituted fault gouge sample from the AG-10 well has a larger range of particle size ranging from 0.4 to 3600 μm, with 490 μm in average. It comprises mostly coarse material (43.2% sand and 30.8% fine-grained gravel size particles) with 9.2% of clay and 16.8% of silt size particles as minor constituents. The particle size distribution curves (Fig. 3), show that the two materials differ both in particle size and distribution. A steep *S*-shaped curve for the calcilutite sample indicates it is well graded (Fig. 3(b)). The flatter, irregular curves of the full fault gouge (Sulem) suggest a large range of particle sizes, poorly graded. However, the fault gouge distribution is multimodal (Fig. 3(a)), and one would expect the hydraulic behaviour to be dominated by the finest fractions, with coarse materials increasing flow tortuosity through bulk samples.

X-ray diffraction analysis revealed that the calcilutite sample is composed mostly of calcite (Table 1). This result is compatible with the limestone bedrock as a source of sediments (50% of calcite, 35% quartz, 15% of albite, and traces of dolomite, muscovite, and clinochlorite). However, the fault gouge obtained from the AG-10 wellbore consists mostly of quartz,

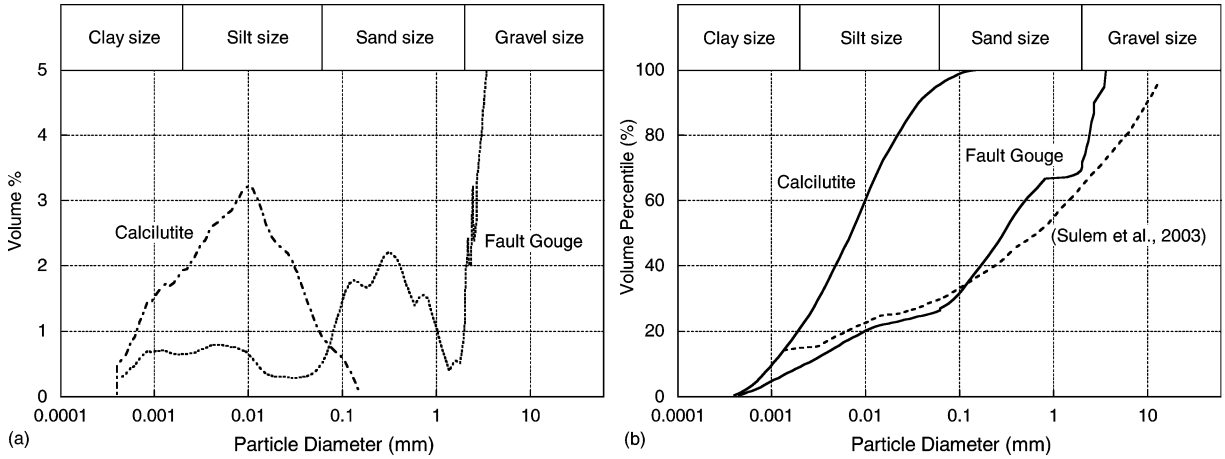

Fig. 3. Particle size distribution of samples in terms of (**a**) volumetric percentage and (**b**) cumulative volumetric percentile for calcilutite, reconstituted AG10 fault gouge, and original fault gouge [7].

Fig. 3. Distribution granulométrique des échantillons en termes (**a**) de pourcentage volumétrique et (**b**) de percentile volumétrique cumulatif pour la calcilutite, la brèche de la faille AG 10 reconstituée, ainsi que pour la gouge de faille originelle.

Table 1
Mineral composition of samples

Tableau 1
Composition minéralogique des échantillons

Mineral	Calcite	Quartz	Albite	Kaolinite	Illite	Smectite	Total
Calcilutite	82	10	2	1	3	2	100 [%]
Mineral	Quartz	Hematite	Albite	Muscovite	Chlorite	others	Total
Fault gouge	70	7	10	12	1	–	100 [%]

Table 2
Physical properties of dry sample after testing

Tableau 2
Propriétés physiques de l'échantillon sec après les tests

Test No.	Diameter [mm]	Length [mm]	Volume [mm^3]	Weight [N]	Unit weight [kN m^{-3}]	Porosity ϕ [%]	Void ratio e (V_v/V_s)
Calcilutite	38.2	32.2	36.9	0.612	16.6	36.9	0.58

as shown in Table 1, related to its origin from cataclasis of radiolarian chert. After the consolidation and the permeability tests, the dimensions and wet and dry weights of the calcilutite sample were measured. The result is shown in Table 2. Based on the phase relationships between the measured unit weight and the calculated unit weight from the average of specific gravity [6], we obtained void ratio (e) and porosity (ϕ) as 0.58 and 36.9%, respectively, for the calcilutite sample. Data for the initial fault gouge values were taken from Sulem et al. [7] with kind permission, with void ratio (e) and porosity (ϕ) of 0.32 and 24%, respectively.

4. Mechanical behaviour

An important mechanical property of fine-grained materials is the time-dependent deformation induced by a sudden change of external load. This transient reaction arises from drainage or suction of pore fluid due to the sudden change of pore volume, and continues until the pore pressure excess or deficit has dissipated [5]. In our experiments, we first observed the drained consolidation behaviour, a transient volume reduction resulting from a sudden increase of external load, at several different vertical stress levels. Shown in

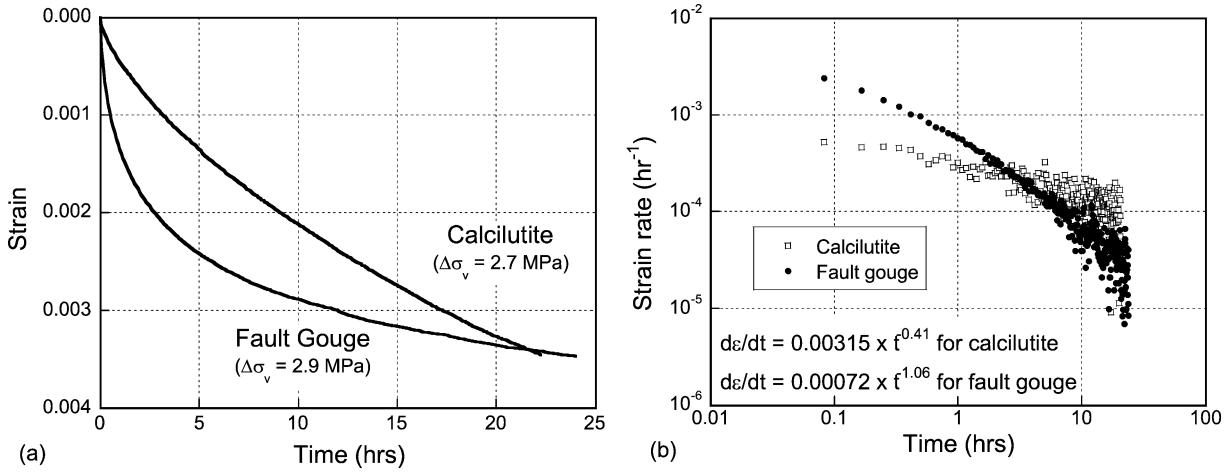

Fig. 4. Consolidation (oedometer) test results of (**a**) strain versus time and (**b**) strain rate versus time under constant uniaxial stress for fault gouge (21.6 MPa) and calcilutite (16.2 MPa). The power regression was taken from data after 1 h.

Fig. 4. Résultats des tests de consolidation (oedomètre) : (**a**) déformation en fonction du temps, sous contrainte uniaxiale constante, pour la brèche de faille (21,6 MPa) et la calcilutite (16,2 MPa). La régression de puissance est issue des données après 1 h.

Fig. 4(a) are typical examples of time-based records of axial strain, equivalent to volumetric strain in our test condition, for the first 24 h. The compaction curves show that strain rate decreases with time for both samples. However, although the calcilutite is initially stiffer than the siliceous gouge, strain rate decreases far more rapidly in the gouge, so that after 22 h the gouge is rapidly stabilising, while the calcilutite continues to compact. This distinctive behaviour can be also expressed in the form of the strain rate change as a function of time, as shown in Fig. 4(b). The strain rate against time is approximated for calcilutite by a bi-linear function in the double logarithm domain with a negative slope. The gouge shows the same relationship, but with a less pronounced transition.

It is instructive to consider the pore volume evolution of the samples. From the consolidation theory [9], the volume of void is a function of fluid pressure dissipating with time, whilst the volume of solid is an elastic response to effective volumetric stress on particles. The variation of void ratio during consolidation at a constant effective volumetric stress was calculated from the axial strain using back calculations from the void ratio measured after testing [2]. Fig. 5 is the cumulative consolidation curve of the calcilutite sample in terms of the void ratio reduction, showing the first 24 h of each one of the five step increases in vertical loading. (The second 24 h of each step were spent in permeability measurement). The rate of void ratio reduction ($-\mathrm{d}e/\mathrm{d}t$) for each level of the vertical stress was plotted in a double logarithm domain in Fig. 5(b). These plots show that the first compaction stage, to 16.2 MPa, causes maximum perturbation in the calcilutite sample. Subsequent load increases yield a separate family of curves. Each curve is approximated by a bi-linear function in the double logarithm domain, with a decreasing slope for increasing vertical stress, except for the final load. The intersection between different slopes is located around an hour after test commencement. At the final loading, 27 MPa, increasing rate of void ratio reduction signals the onset of pervasive grain crushing in the sample.

Fig. 6 is the full data set of compaction data illustrating the significant behaviour difference between calcitic mud, and siliceous fault gouge. In calcilutite, the first step of load increasing (16.2 MPa) led to a large consolidation with a clear change in volume reduction rate, but each subsequent 2.7 MPa load increase produced much lower consolidation with only gradual stiffness increase. In the fault gouge, 3 MPa compaction steps show rapid stiffness increase with time.

A notable feature of the data are minor discontinuities, arrowed in Fig. 6(b), in the fault gouge

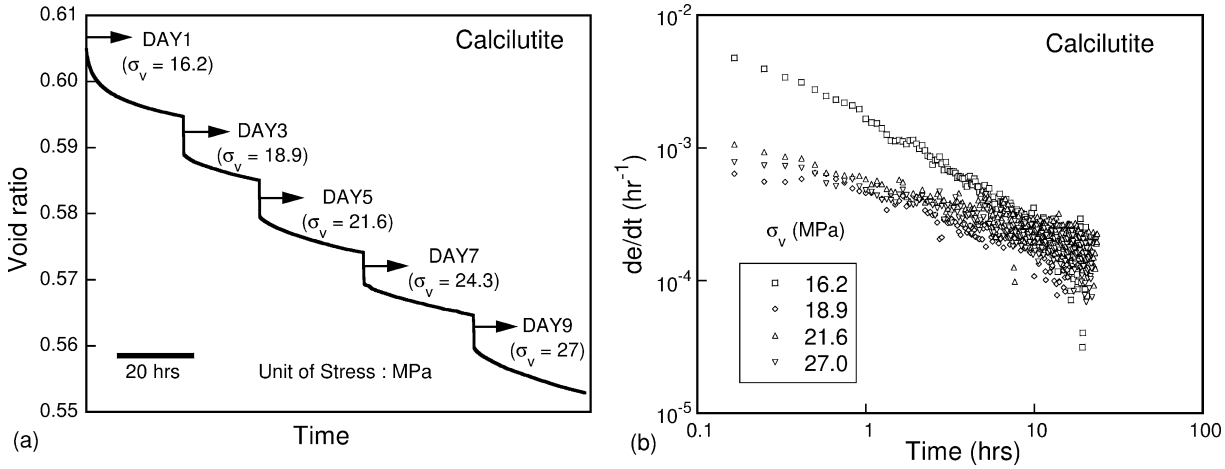

Fig. 5. (**a**) Time-based record of consolidation in terms of the void ratio (e) reduction at five different uniaxial stress levels. (**b**) Rate of void ratio reduction ($-\mathrm{d}e/\mathrm{d}t$) as a function of time showing bi-linear behaviour.

Fig. 5. (**a**) Enregistrement en fonction du temps de la consolidation en termes de réduction du rapport de vide (e) à cinq différents niveaux de contrainte uniaxiale. (**b**) Taux de réduction du rapport de vide ($-\mathrm{d}e/\mathrm{d}t$) en fonction du temps, mettant en évidence un comportement bi-linéaire.

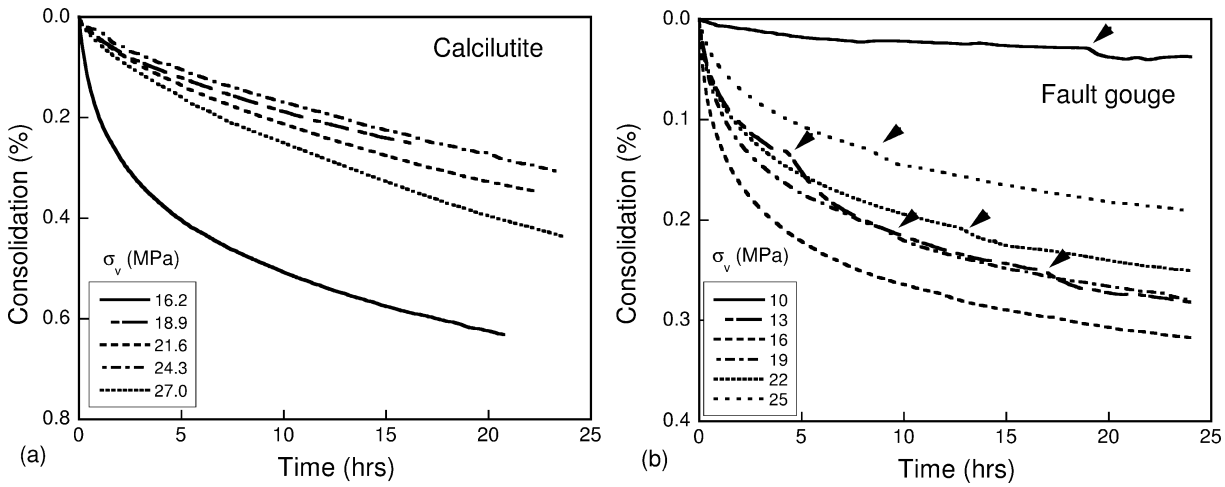

Fig. 6. Consolidation curves at different levels of vertical stress for (**a**) calcilutite and (**b**) fault gouge samples. Arrows indicate sudden changes in consolidation curves due to the subtle change in the vertical stress.

Fig. 6. Courbes de consolidation à différents niveaux de contrainte verticale pour les échantillons de calcilutite (**a**) et de gouge de faille (**b**). Les flèches indiquent des changements brutaux dans les courbes de consolidation, dus au changement ténu dans la contrainte verticale.

compaction curves, missing in the calcilutite curves. These are traceable to minor changes in applied load arising from slight temperature sensitivity of the load frame gas pressure buffers. An example of a correlation between the subtle change (less than 1.5%) of vertical stress and the sudden change in consolidation curve (about 10%) in Fig. 7 shows that transient compaction is extremely stress-sensitive in the siliceous fault gouge. This implies that stress transmission through the gouge is extremely inhomogeneous, with distinct volumes always lying close to critical collapse strength.

Because the hydraulic properties of the materials are of importance, the volumetric reduction with time

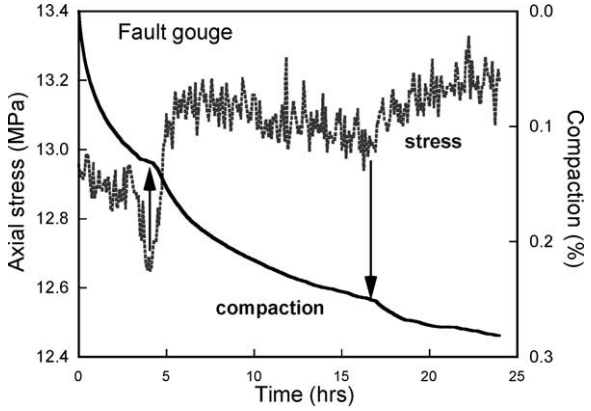

Fig. 7. Axial stress-dependent compaction curve.

Fig. 7. Courbe de compaction dépendant de la contrainte axiale.

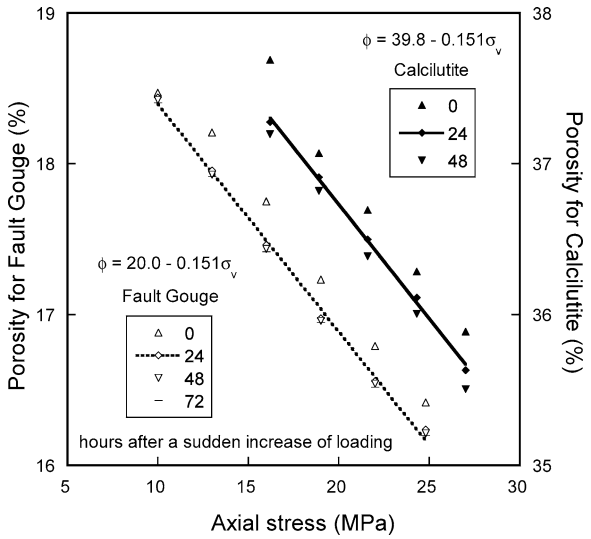

Fig. 8. Linear relationship between porosity reduction and axial stress. The number after each symbol means hours elapsed after a sudden change in axial load.

Fig. 8. Relation linéaire entre réduction de porosité et contrainte verticale. Le nombre après chaque symbole représente les heures écoulées après un changement brutal dans la charge axiale.

for each level of the axial stress was converted into the variation of porosity as a function of the axial stress (Fig. 8), using consolidation theory [9]. Because the porosity is also a function of time, we plotted in Fig. 8, the porosity data at different times elapsed after the change of axial stress: 0, 24, and 48 h for calcilutite, and 0, 24, 48, and 73 h for fault gouge. We find that porosity at a given time is a linear function of external stress in both samples, with the same dependency, but different zero intercept.

5. Hydraulic characteristics

Permeability evolution with compaction was measured by pumping degassed-deionised water upward through the sample at constant low flow-rate (1.05×10^{-10} $m^3 s^{-1}$ for calcilutite and 4.2×10^{-11} $m^3 s^{-1}$ for fault gouge), after the one-day drained consolidation interval at each load step. The evolution of differential fluid pressure across the samples is shown in Fig. 9.

Calcilutite and fault gouge had very different hydraulic responses. The calcilutite, which is a well-sorted granular powder with low clay content, showed a steady pressure rise for the first 15 h toward a plateau value. In contrast, the gouge, which is a poorly sorted powder with moderate clay content, showed a rapid pressure rise, until establishment of an irregular fluctuating differential pressure. The rate of initial pressure rise is load dependent.

Permeabilities were estimated using Darcy's law with an assumption that the stabilised upstream pressure at each vertical stress level comes from a steady-state condition of flow. The evolution of permeability versus porosity is usually expressed in the literature in a double logarithm domain, as shown in Fig. 10. Both samples are approximated by a linear function in such a scale. The relationship between permeability and porosity of calcilutite and fault gouge are compatible with other silt-size mud-rich slurries in the literature [2], except for the horizontal shift due to particle size differences.

The different pressure rise behaviour of the calcilutite and gouge has important implications for the sealing style and evolution of the cap rock and fault filling they represent. The regular slow pressure rise in the calcilutite implies that this material, and by implication, all limestone gouges, act as homogeneous materials, transmitting water by homogeneous plug flow. Thus the permeability measured in the compaction studies detailed above is a true bulk property of the material. Hence the expected sealing capacity of the caprock or fault gouge can be calculated by direct spatial scaling from the experimental data. In contrast, the siliceous fault gouge, perhaps because of poor sort-

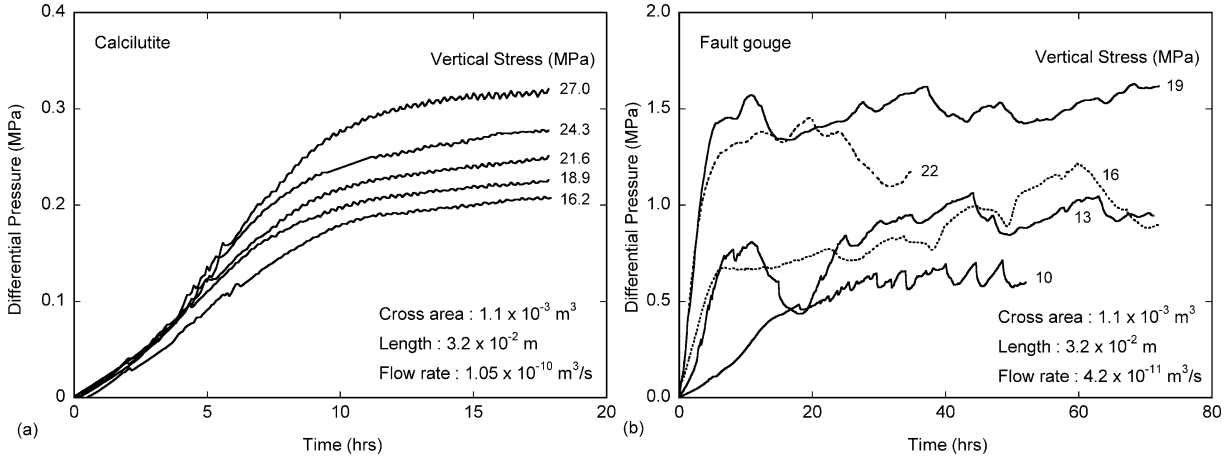

Fig. 9. Time-dependent variation of differential pressure along (**a**) cacilutite and (**b**) fault gouge. Note that the flow rate for fault gouge under 16 MPa vertical stress was reduced to 2.1×10^{-11} $m^3 s^{-1}$.

Fig. 9. Variation dépendant du temps de la pression différentielle le long de la calcilutite (**a**) et de la gouge de faille (**b**). À noter que le débit pour la gouge de faille, sous contrainte verticale de 16 MPa, a été réduit à $2{,}1 \times 10^{-11}$ $m^3 s^{-1}$.

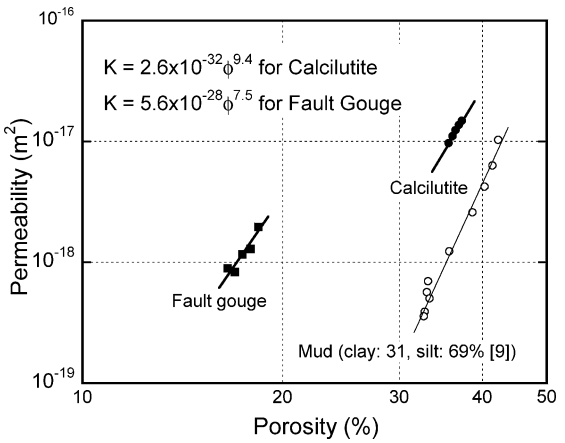

Fig. 10. Variation of permeability as a function of porosity in a double-log domain, showing a linear relationship in each sample.

Fig. 10. Variation de la perméabilité en fonction de la porosité dans un domaine bi-logarithmique montrant une relation linéaire pour chaque échantillon.

ing, but more probably, because of the clay content, exhibits two permeabilities. The extremely rapid initial pressure rise at flow commencement indicates that the 'static' permeability of the gouge is extremely low. However, the sudden establishment of a fluctuating, irregular differential pressure under low flow conditions indicates that there is a 'breakthrough' differential pressure, which represents the onset of 'packet' flow through local inhomogeneities in the gouge. This local nature of permeability in the gouge correlates with the extreme local stress sensitivity of the material, noted in Section 4. Thus the measured *flow* permeability is not expected to scale spatially, but probably represents an absolute property of this type of gouge. It is notable that the fluid pressure measured below the gouge in the actual borehole is 1 MPa, which is predicted from the flow data in Fig. 9.

6. Conclusions

Two important poorly consolidated units from the Aigion Fault area have been characterised in terms of hydraulic and mechanical behaviours. One, a calcilutite, is a common fine-grained calcitic cap formation between the basal limestones and overlying conglomerates. This unit is important as a potential topseal to the limestone, and because it is a good analogue for limestone-derived fault gouge. The other is siliceous active fault gouge from the AG-10 well, a cataclasite derived from radiolarian chert. For mechanical deformation, both samples show a clear transient behaviour for a sudden change in external loading. However, calcilutite is more time-dependent, and fault gouge is more pressure-dependent, and the latter is notably sensitive to small perturbations in loading. For hy-

draulic characteristics, both have low, load-dependent permeability, 9–15 $\times$ 10^{-18} m^2 for the calcilutite and 0.9–2 $\times$ 10^{-18} m^2 for the fault gouge. Hence both are flow sealing compared to the heavily fractured limestone bedrock in the area. However, values for the calcilutite are shear-insensitive global values, whereas those for the siliceous gouge are local limits under cross-flow, and must be shear rate sensitive. We conclude transient response to sudden changes in effective stress may play a crucial role in the time-dependent triggering of fault movement in the Aigion region.

Acknowledgements

The work was funded by EU 5th Framework projects EVR1-CT-2000-40005 (DGLab-Corinth) and ENK6-CT-2000-00056 (FFF-Corinth). The calcilutite sample was recovered from a short field trip to the Gulf of Corinth. We acknowledge the assistance given to us by Isabelle Moretti, Ioannis Vardoulakis, and the FFF team. Especial thanks are due Jean Sulem and colleagues at CERMES.

References

[1] A. Avallone, P. Briole, E. Papazissi, C. Mitsakaki, D. Paradissis, H. Billiris, Analysis of Eleven Years GPS Data in the Gulf of Corinth, EGS2002, Nice, 2002.
[2] M.A. Biot, General theory of three-dimensional consolidation, J. Appl. Phys. 12 (1941) 155–164.
[3] R.F. Craig, Soil Mechanics, Chapman & Hall, London, 1997.
[4] R.E. Goodman, Introduction to Rock Mechanics, Wiley, New York, 1989.
[5] I.K. Koukouvelas, The Egion fault, earthquake-related and long-term deformation, Gulf of Corinth, Greece, J. Geodyn. 26 (1998) 501–513.
[6] I. Moretti, L. Micarelli, J.-M. Daniel, S. Eyssauttier, C. Frima, The Cores of AG-10, Report 57 240, February 2003, Institute Français du Pétrole, 2003.
[7] J. Sulem, I. Vardoulakis, H. Ouffroukh, M. Boulon, J. Hans, Experimental characterization of the thermo-mechanical behaviour of the Aigion fault gouge, C. R. Geoscience 336 (2004) 455–466, this issue.
[8] T. Tokunaga, S. Hosoya, H. Tosaka, K. Kojima, An estimation of the intrinsic permeability of argillaceous rocks and the effects on long-term fluid migration, in: S.J. Düppenbecker, J.E. Iliffe (Eds.), Basin Modelling: Practice and Progress, in: Geol. Soc. Lond., Spec. Publ., vol. 141, 1998, pp. 83–94.
[9] R. Westaway, The Quaternary evolution of the Gulf of Corinth, central Greece: coupling between surface processes and flow in the lower continental crust, Tectonophysics 348 (2002) 269–318.